Sensors & Transducers, Vol. 172, Issue 6, June 2014, pp. 13-20

Sensors & Transducers

Design of Temperature Compensation Module of the Industrial Robot Wrist Force Sensor Based on Multivariate Regression Method

[1] Yuan Chuanlai, [2] Zhang Yueyi, [1] Xiao Shenping, [1] Kong Lingshuang
[1] College of Electrical and Information Engineering, Hunan University of Technology, Zhuzhou, 412000, China
[2] Changsha Vocational & Technical College, Changsha, 410111, China
Tel.: 13873395945

Received: 11 April 2014 /Accepted: 30 May 2014 /Published: 30 June 2014

Abstract: This paper takes software method to compensate temperature against the drift problem of piezoresistive waist force sensor. The compensation algorithm is modeled through using the PLS method. And compensation module is designed based on multiple regression method. According to the simulation results, the system designed meet the basic phenomenon for drift correction. Finally, the actual data is used to validate this algorithm. *Copyright © 2014 IFSA Publishing, S. L.*

Keywords: Wrist force sensor, Temperature compensation, PLS modeling, Multivariate regression.

1. Introduction

Along with the rapid development of modern detection techniques, the application of piezoresistive wrist force sensors in industrial production practice is more and more wide. In the twenty-first century, modern scientific and technological revolution is to come. The sensor technology has attracted wide degree attention of domestic electronic information industry. It can even be said that the technical level of sensors is one of the important criteria to measure the level of a national science and technology.

In recent years, the development of foreign wrist force sensor compensation technology is very quickly, and the development direction is committed to intelligence, miniaturization, integration, and digital. In order to correct and compensate for the sensor, many companies have launched internal integrated intelligent signal conditioning chip within the wrist force sensor to compensate for the imbalance, temperature drift and non-linearity and other parameters. The computer system is also used to achieve correction and compensation of sensor. This method has high compensation accuracy, stability, small size and is easy to transport. The main bottleneck of piezoresistive wrist sensor in practical process is the temperature drift problem. Since the birth day of piezoresistive wrist sensor, the study of temperature drift compensation has begun, compensation is also developed from the hardware to the software compensation stage.

Software compensation can achieve high compensation accuracy, high accuracy and linearization of digital circuits, and can also promote the development of sensor temperature compensation technology. Software compensation technology is relatively simple, and the compensation effect is obvious, it is an important way to improve the accuracy of wrist force sensor. So, most of modern popular wrist sensor temperature compensation are the software compensation methods.

American psychologist Charies Spearman proposed PCA (also known as factor analysis method) in 1904, then Hotelling has improved and developed a multivariate statistical analysis method, it has reduced system dimension and principal component extraction characteristics. Successively, B. M. Wise [1] and other scholars have applied the method to process monitoring fields. The multivariate statistical process control (MSPC) theoretical framework proposed by J. F. MacGregor combines the kinds of statistical analysis methods PCA and control theory and promotes the multivariate statistical methods further applications in industrial processes [2-5]. The major step of principal component analysis (PCA) is the principal component extraction which mines and analyses multivariate historical data to extract the finite element main variables. Principal component analysis can reduce high-dimensional data dimensionality to avoid loss of data. And it makes it simple and easy to operate data analysis [6-7]. Original data can be converted by the data space (p1 and p2 direction vector) that is the projection by the projection vector to obtain a new variable (Fig. 1) and then form the main component vector, this method is the principal component extraction. So far, the principal component extraction method has been able to adapt to the dynamic process and non-linear process.

2. The Structure of Industrial Robot Wrist Force Sensor

This section describes the basic structure of an industrial robot common wrist force sensor, and finds the drift of the sensor accuracy and sensitivity in the structure.

2.1. System Architecture of Wrist Force Sensor

As is shown in Fig. 1, an industrial robot wrist force sensor is mainly composed of the following two parts:

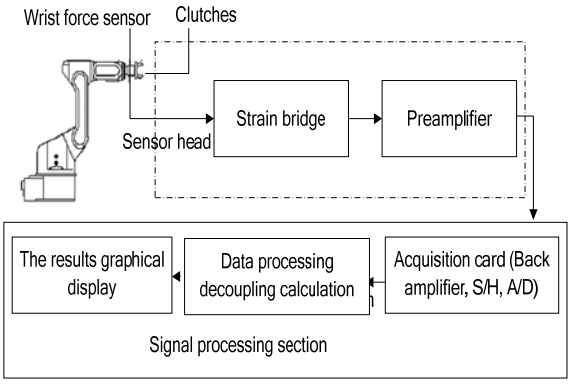

Fig. 1. System diagram of wrist force sensor.

1) Sensor head section. The section mainly includes pressure strain body, strain bridge and preamp, etc. The force signals could be converted into electrical signals which can also be pre-amplified.

2) Signal processing section. This part is mainly for amplification, signal filtering, A/D conversion, while the other information is sent to the computer for data and temperature compensation process. The signal processing portion has a stronger processing capability to optimize complex algorithms, and achieve the microcomputer control, etc.

2.2. The Mechanical Structure of Wrist Force Sensor

This paper takes the cross beam type wrist force sensor as example to describe the basic mechanical structure of wrist force sensor.

Cross beam type sensor have a pair of elastic strain gauges in the front and back wrist and two side beams each. The strain gauge position of the wrist force sensor is shown by Fig. 2. The strain gauges attach to the cross beam near the center part in medial patch mode, and the principle of the patch position selection is high sensitivity, greater resolution, small dimension between interference.

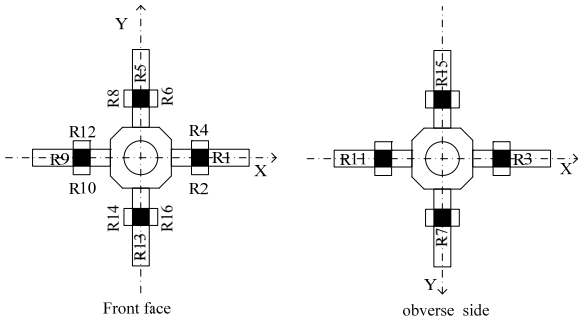

Fig. 2. Cloth diagram of cross elastic beam.

2.3. The Circuit Structure of Wrist Force Sensor

Equivalent bridge configuration of wrist force sensor is shown in Fig. 3, when the strain gauge is under pressure, the two sides are also under the pressure at the same time, the resistor of a opposite sides increases/ decreases, the other sides' decreases / increases.

Assuming that the input voltage is Ui, the output voltage is Uo, according to the principle of the bridge, the relationship between them is shown in Equation 1.

$$V_O = \frac{\left[(R_1+\Delta R_1)(R_3+\Delta R_3)-(R_2-\Delta R_2)(R_4-\Delta R_4)\right]}{(R_1+R_2+\Delta R_1-\Delta R_2)(R_3+R_4+\Delta R_3-\Delta R_4)} \quad (1)$$

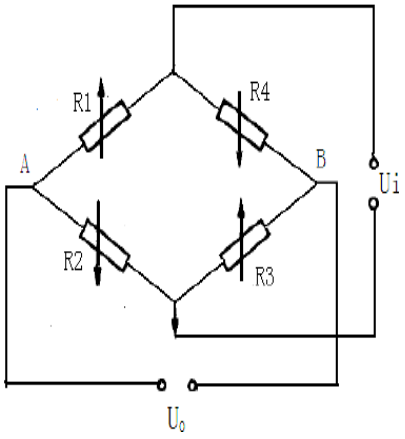

Fig. 3. Bridge circuit of wrist force sensor.

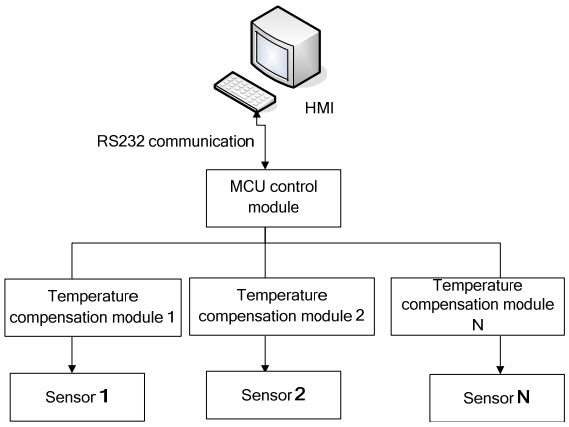

Fig. 4. System architecture of temperature compensation.

From Equation 1, wrist force sensor is mainly based on the change in resistance strain gauges to calculate the size of the pressure. When the temperature changes, the resistance value will change, and this will affect the accuracy and sensitivity of the sensor.

Thus, the bridge output change is mainly caused by the change in resistance. Simplify the formula, ignore the change in resistance, the quadratic is:

$$U = U_p = U_i \frac{(R_1R_3 + R_2R_4)}{(R_1 + R_4)(R_2 + R_3)} \frac{2\Delta R_i}{R_i} = U_i \frac{2(R_1R_3 + R_2R_4)}{(R_1 + R_4)(R_2 + R_3)} \pi\sigma \quad (2)$$

Among (2) $\frac{\Delta R_i}{R_i} = \pi\sigma$

As can be seen from Equation 2, the main cause of sensitivity variation is piezoresistive coefficient [8-10]. There are two main factors affecting the piezoresistive coefficient: the diffusion impurity concentration and ambient temperature. When the diffusion impurity concentration increases (decreases), the piezoresistive coefficient decreases (increases). And when the surface impurity concentration is low, the temperature increases, the piezoresistive coefficient decreases fastly; when the surface impurity concentration is high, the temperature increases, the piezoresistive coefficient decreases slowly. While reduce the temperature, increase the diffusion impurity concentration, the piezoresistive coefficient will also be reduced, and the output sensitivity is affected.

2.4. Temperature Compensation Module Analyze

As is shown in Fig. 4, the system uses lumped control architecture, each wrist force sensor is equipped with a temperature compensation module. Each temperature compensation module which is connected to the MCU control module via the bus way is eventually sent to the man-machine interface through the serial port.

3. Temperature Compensation Module Based on Multivariate Regression Method

Multiple linear regression, whose optimization goal is that the sum of absolute errors of dominant variable is minimal, analyzes the auxiliary variable through linear regression method. Multivariate statistical analyze theory is through a large number of historical and current data, establish statistical analysis model of the process variables and the main factor variables, whose modeling process is relatively simple, model structure is unified, and the design of overall system is easy. The main thing is that the method is tried in high-dimensional complex object model, and can establish high precision linear or nonlinear models.

3.1. Multiple Regression Method

PCA method is based on the variance of the data changes as an indicator to determine the corresponding direction variable of the PCA variable. The historical data could be extracted effectively and dimension is also reduced through the vector transformation and solving. The basic idea of PCA method is: Find a new set of variables which is a linear combination of the original variable instead of the original one. From the perspective of optimization, principal component variables, whose number is fewer than the original variables, can carry the useful information of the original data to the largest extent and are unrelated between themselves. It includes the definition and acquisition of the principal component, as well as the data reconstruction. It belongs to the category regression method, but it does not show a nonlinear relationship model. So far, PCA methods are emerging in endlessly, such as: KPCA, NPCA and so on. The kernel principal component analysis (KPCA) has attracted widespread attention of scholars in recent years, the variable is transformed into a high-dimensional space by nonlinear mapping, and the

most important information in the data is contained to the first principal component variable, so KPCA is a simple and effective nonlinear PCA method.

PLS algorithm as a multivariate linear regression technique was first proposed and used in the field of economics to deal with the high-dimensional data by scholar Wood. Unlike PCA algorithm, while PCA extraction, the internal model relationship of principal component input and output variables is established, it can render the external physical contact between variables of system. PLS combines the PCA with canonical correlation analysis and inherits characteristics of both algorithms, so it reduces dimensionality and establishes the characteristic relationship between input and output variables of the model. In the PLS, through using the principle of maximizing the covariance, solve the principal component which could reflect the relationship between the input and output variables successively, the principal component extraction and model regression are simultaneous in the process. Typically, PLS model consists of two parts, i.e. the internal model and external model, characterize regression process and principal component extraction process respectively. Wherein the external model

$$X - E^* = \sum_{i=1}^{R} t_r p_r^T = TP^T \tag{3}$$

$$t_r = h_r(\ddot{t}_r) \quad T = XW \tag{4}$$

$$Y - F^* = \sum_{i=1}^{R} u_r q_r^T = UQ^T \tag{5}$$

$$U = YC \tag{6}$$

From the Formula 3-6, it can be seen that the original high-dimensional data matrix can be decomposed into the sum of the vector product. Where E *, F * represent the residual matrix after principal component extraction. Tr, pr are the r^{th} input principal component and load vector; T, P are the implicit variable matrix and direction matrix for response; Ur, qr represent r^{th} output principal component and load vector; U, Q are corresponding matrix form; W, C are input and output projection vector respectively.

The internal model is obtained by linear regression of T and U

$$\hat{U} = TB \tag{7}$$

So, the PLS model formula is:

$$Y = UQ^T + F = TBQ^T + F^* \tag{8}$$

PLS control diagram is shown in Fig. 5.

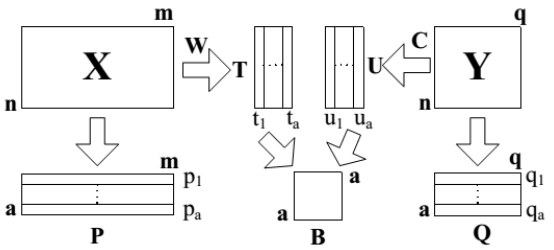

Fig. 5. PLS control block diagram.

3.2. The Application of Multiple Regression Method in the Temperature Compensation

In this paper, multivariate regression method is designed for the wrist force sensor stress chip temperature compensation. If the experimental method is adopted, in the range of -40 ºC~125 ºC, the various temperature compensation coefficients are measured to establish the input and output data sets. Under normal circumstances, the limited discrete points are selected to correct the wrist force sensor, and then we record compensation coefficients on these points, get compensation coefficient at each temperature by using the software method.

In the standard PLS, a given process data are often divided into two data blocks, the dependent variable data $X=(x_{ij})_{1Xm}$ and the independent variable data $Y=(y_{ij})_{1Xn}$, i.e. input and output data of the system, l, m, n denote the observation number, the dimension number of input and output variable. External model can extract the principal component through iterative calculation of input data X and output data Y, as is shown in Equation 5.

The internal model of PLS algorithm characterizes the mathematical relationship between the input principal component variable t_r and output principal component variable u_r:

$$b_r = u_r^T t_r / t_r^T t_r \tag{9}$$

$$u_r = b_r t_r \tag{10}$$

where F* is the modeling error, b_r is the regression parameter of the r^{th} principal component variable space, the principal component spatial regression matrix B characterizes the correlation degree between the data in the projection space. The traditional PLS modeling method often ignores the dynamic characteristics of system that is the dynamic model relationship, but merely indicates steady-state relationships between data. Therefore, many scholars introduce the dynamic characteristics model establishment into PLS algorithm as improvement for this deficiency.

The dynamic relationship of internal model within the PLS model proposed by Ray and Kasper can express approximately the mathematical description

of dynamic filter added before PLS modeling. Assuming H(*) is filter model added before the PLS modeling, the data $\widetilde{E}$ is obtained through adding filters on the basis of the steady-state model, that is:

$$\tilde{E}_r = H(E_r), \tag{11}$$

where E_r is the residual matrix after the r^{th} step principal component extraction, the direction vector, which is used at r step principal component extraction, is obtained by solving the largest eigenvalue. At this time, the parameters of the PLS are:

$$\begin{aligned} w_r &= \text{vector}_{\lambda max}(H(E_{r-1}^T)F_{r-1}F_{r-1}^T E_{r-1}^T \ , \\ t_r &= \tilde{E}_r w_r = H(E_{r-1})w_r , \\ p_r &= H\left(E_{r-1}^T\right)t_r / t_r^T t_r , \end{aligned} \tag{12}$$

where H (*) which is a diagonal matrix can be transformed into the internal model filter $h_r(*)$ in each principal component variable space. Through the matrix transformation, the Equation 12 can be expressed as:

$$\begin{aligned} \ddot{t}_r &= h_r^{-1}(t_r) = E_{r-1}w_r \\ t_r &= h_r(\ddot{t}_r) \end{aligned} \tag{13}$$

Among them, the projection of primitive variable in vector w_r is t_r, the projection of dynamic data in the w_r after adding filter is t_r. Therefore, the internal model in the dynamic PLS model can be expressed approximately as a combination of filter model and static PLS internal model. At this time, the structure of dynamic external model in the PLS model can be expressed as:

$$Y - F = H\left(\ddot{T}\right)BQ^T = H(E_0W)BQ^T \tag{14}$$

The dynamic characteristic of the system is obtained by introducing the filter in each principal component variable space. In order to describe the dynamic characteristic of the system better, this paper combines auto-regression model ARX with PLS to characterize the dynamic characteristics of the system through applying ARX model into the dynamic description in internal model of PLS, at this time, it becomes ARX-PLS model. The representation of this dynamic PLS internal model is:

$$\begin{aligned} u_r &= H_r(t_r) \\ Y - F &= H(T)Q^T = \sum_{r=1}^{R} H_r q_r^T \\ H(T) &= \text{diag}(H_1(t_1), \ldots, H_R(t_R)) \end{aligned} \tag{15}$$

Among (15), $H_r(t_r)$ is the dynamic model of r^{th} sub-system with linear ARX form in hidden variable space. The system can be broken down into separate small systems to facilitate algorithm design through this method. However, the specific identification method of the system needs further introduction.

Combining the model expressed by Equation 15, the optimization proposition of original spatial variables is put forward:

$$\min J_O = \frac{1}{2}\sum_{k=1}^{n}\left(y(k) - y^{PLS}(k)\right)^T\left(y(k) - y^{PLS}(k)\right) \tag{16}$$

$y(k)$ and $y^{PLS}(k)$ are original output and the output obtained by ARX-PLS modeling at time k respectively. However, the proposition is expressed the optimization proposition of principal component output variable:

$$\min J = \frac{1}{2}\sum_{k=1}^{n}\left(u(k) - u^{PLS}(k)\right)^T\left(u(k) - u^{PLS}(k)\right) \tag{17}$$

$u(k)$ and $u^{PLS}(k)$ are the output of principal component and ARX-PLS internal model at time k respectively.

$$\begin{aligned} u(k) &= [u_1(k), u_2(k), \ldots, u_R(k)] \\ u^{PLS}(k) &= [u_1^{PLS}(k), u_2^{PLS}(k), \ldots, u_R^{PLS}(k)] \end{aligned} \tag{18}$$

Thus, the optimization proposition of the Formula (18) can be substituted for:

$$\min J = \frac{1}{2}\sum_{r=1}^{R}\sum_{k=1}^{n}\left(u(k) - u^{PLS}(k)\right)^2 = \min J_1 + \min J_{2+\ldots+} \min J_r + \min J_R \tag{19}$$

Among: $J_r = \frac{1}{2}\sum_{k=1}^{n}\left(u(k) - u^{PLS}(k)\right)^2$

$u_r(k)$ and $u_r^{PLS}(k)$ are the output of r^{th} dependent variable subspace and the corresponding ARX. The input and output in the principal component variable space in the ARX model at time k are:

$$u_r^{PLS}(k) = \varphi_r(k)\theta_r(k) \tag{20}$$

$\varphi_\rho(k) = [u_r(k-1), u_r(k-2), \ldots,$
$u_r(k-n), t_r(k-d-1),$
$t_r(k-d-2), \ldots, t_r(k-d-m)]$ include the current and historical information of input and output variables in the r^{th} principal component variable space, wherein d_r is the lag time coefficient of subsystem, m, n are the input and output order of the various subsystems.

$\theta_r(k)=[-a_{r1}(k),-a_{r2}(k),\ldots,-a_m(k),$
$-b_{r1}(k),-b_{r2}(k),\ldots,-b_m(k)]^T$ include the regression parameters of the r^{th} hidden variable ARX model at time k, the proposition on the subsystems is:

$$J_r=\frac{1}{2}\sum_{k=1}^{n}\left(u(k)-u^{PLS}(k)\right)^2=\frac{1}{2}\sum_{k=1}^{n}\left(u_r(k)-\varphi_r(k)\theta_r(k)\right)^2 \quad (21)$$

The parameters are obtained using the system identification method [11-12] for proposition, that is:

$$\theta_r(k)=(\varphi_r^T(k)\varphi_r(k))^{-1}\varphi_r^T(k)\theta_r(k) \quad (22)$$

The parameters m, n and d_r have been pre-determined before parameter identification of the ARX-PLS model.

4. The Simulation Results

4.1. Performance Index

The sensitivity of wrist force sensor is impacted by temperature greatly. The coefficient of thermal sensitivity is used to compare forth with back temperature compensation effect of the sensor. Accuracy is expressed as the size of measurement data error of wrist force sensor in the whole size range.

The coefficient of thermal sensitivity drift is defined as:

$$K_s\frac{Y_f(T_i)-Y_0(T_i)-Y_f(T)-Y_0(T)}{(T_i-T)Y_f(T)-Y_0(T)}\times 100\%\frac{FS}{^\circ C} \quad (23)$$

$Y_f(T_i)$ - the corresponding output to full-scale value of wrist force sensor at the temperature of T_i. The accuracy, which is the percentage of the maximum absolute error of the sensor under predetermined condition with respect to measurement range, is typically used to indicate the relative value of measurement error. And it is defined as:

$$A=\frac{\Delta A}{Y_{F.S}}\times 100\% \quad (24)$$

Among (24), ΔA represents the allowable absolute maximum error in the measurement range, $Y_{F.S}$ means the full-scale output.

4.2. Experimental Data

Because of equipment limitation, this article does not carry out the measured data. The comparative data used for the validation experiments of the algorithm is performance and measurement accuracy data of test sensors which are the two PA-10 types Keller wrist force sensor from precision instrument and optoelectronics engineering of Tianjin university within -40-100 °C range for compensation and 0-20 kPa for the sensor range. Take eight test points from -40 °C~100 °C temperature range to take: -40 °C, -30 °C, -15 °C, 0 °C, 20 °C, 50 °C, 70 °C, 100 °C. Set five points within each cycle test points, keep applying pressure more than 30 seconds on each pressure point and then measure the output of the sensor with voltmeter. The test results of the sensor are shown in Table 1 and Table 2.

Table 1. The test data sheet of sensor A.

Temperature	-40	-30	-15	0	20	50	70	100
Compensation Value	-5.6	-4.8	-3.73	-2.36	0.74	-5.6	0.99	-0.39
	25.59	26.14	26.78	27.75	31.3	25.59	31.58	31.07
	56.88	57.21	57.41	58.04	61.99	56.88	62.64	61.89
	88.39	88.42	88.14	88.43	92.8	88.39	93.15	92.93
	119.81	119.63	118.95	118.88	123.67	119.81	124.05	124.23
	88.25	88.37	88.19	88.23	92.79	88.25	93.11	92.67
	56.98	57.23	56.1	58.02	61.98	56.98	62.52	61.99
	25.57	26.15	27.78	27.76	31.32	25.57	31.54	31.08
	-5.6	-4.8	-3.7	-2.36	0.79	-5.6	0.91	-0.35

Table 2. The test data sheet of sensor B.

Temperature	-40	-30	-15	0	20	50	70	100
Compensation Value	-20.84	-22.97	-25.56	-26.65	-29.79	-24.67	-23.67	-21.53
	9.08	6.42	3.62	2.25	-0.62	3.62	5.31	7.89
	39.48	35.43	32.89	31.25	29.58	32.09	34.43	37.49
	69.12	65.22	61.73	60.3	58.92	60.62	63.61	66.26
	98.71	95.47	91.51	89.52	89.36	89.32	92.52	95.23
	69.03	65.62	62.47	60.32	58.98	60.62	63.59	66.27
	38.89	35.77	32.82	31.25	29.71	32.07	34.49	37.5
	9.06	6.53	3.59	2.36	-0.45	3.59	5.34	7.82
	-20.82	-22.96	-25.56	-26.61	-29.52	-24.69	-23.67	-21.52

Table 3. The test data sheet of sensor A.

Temperature	-40	-30	-15	0	20	50	70	100
Compensation Value	3.949	3.926	3.924	3.940	3.911	3.925	3.945	3.929
	7.012	7.033	7.004	7.031	7.033	7.036	7.045	7.049
	10.329	10.301	10.306	10.343	10.324	10.342	10.310	10.328
	13.518	13.502	13.524	13.510	13.506	13.510	13.507	13.509
	19.928	19.932	19.921	19.910	19.947	19.904	19.905	19.907
	13.609	13.620	13.607	13.602	13.647	13.615	13.615	13.617
	10.342	10.328	10.343	10.317	10.322	10.303	10.309	10.333
	7.149	7.127	7.135	7.150	7.114	7.121	7.123	7.138
	3.918	3.903	3.926	3.917	3.909	3.910	3.945	3.934

Table 4. The test data sheet of sensor B.

Temperature	-40	-30	-15	0	20	50	70	100
Compensation Value	3.939	3.915	3.930	3.948	3.922	3.935	3.938	3.922
	7.009	7.013	7.040	7.024	7.038	7.020	7.014	7.002
	10.330	10.303	10.316	10.339	10.335	10.306	10.307	10.305
	13.536	13.527	13.505	13.532	13.506	13.507	13.505	13.507
	19.928	19.916	19.908	19.931	19.949	19.909	19.913	19.920
	13.627	13.642	13.630	13.617	13.615	13.623	13.621	13.618
	10.321	10.306	10.301	10.315	10.316	10.333	10.348	10.347
	7.138	7.137	7.137	7.105	7.134	7.123	7.111	7.105
	3.933	3.945	3.926	3.935	3.908	3.948	3.927	3.934

According to the above data, do data modeling based on PLS method. Fig.6 shows the result of the predicted output and the actual output through dynamic ARX-PLS PLS model. It can be seen that there are some errors of the system but the dynamic characteristics of the system can tracked. The PLS modeling parameters are obtained as follow:

$$P = \begin{bmatrix} -0.0311 & -0.2423 & 0.9985 & -0.1724 \\ -0.1953 & 0.5380 & 0.0277 & -0.8360 \\ 0.9545 & 0.1054 & 0.0463 & -0.0732 \\ 0.2231 & -0.8004 & -0.0025 & -0.5157 \end{bmatrix}$$

$$Q = \begin{bmatrix} 0.5941 & 0.9614 & 0.5974 & 0.9452 \\ 0.8044 & -0.2750 & -0.8019 & 0.3265 \end{bmatrix}$$

$$W_x = \begin{bmatrix} 0.2868 & & & \\ & 0.2710 & & \\ & & 0.2446 & \\ & & & 0.2936 \end{bmatrix}$$

$$W_y = \begin{bmatrix} 0.2572 & \\ & 0.2694 \end{bmatrix}$$

The internal model dynamic PLS is gotten through the multiple regression method:

$$H(Z) = \begin{bmatrix} \dfrac{0.0651z - 0.0688}{z^2 - 1.1980z + 0.3112} z^{-1} & \dfrac{0.0024z + 0.0489}{z^2 - 1.4087z + 0.4835} z^{-1} \\ \dfrac{0.0100z + 0.0131}{z^2 - 1.2449z + 0.4061} z^{-1} & \dfrac{0.0015z + 0.0148}{z^2 - 1.2194z + 0.3806} z^{-1} \end{bmatrix}$$

Modeling results are shown in Fig. 7. It can be seen that dynamic compensation model is applied to the sensor temperature compensation to achieve better practical results.

The experimental results analysis:

1) The experiment measured data is obtained in the warming case, the residence time at each measurement point is 30 minutes, this case is consistent with algorithm compensation temperature, the real objective compensation effect can be reflected objectively to a certain extent.

2) It can be found that the algorithm has significant improvement for sensitivity drift by contrasting Zero drift and sensitivity drift data before and after sensor compensation, sensitivity temperature drift error has been reduced on the order of magnitude.

3) The entire compensation circuit is in the -40 °C~100 °C temperature range, the linearity of curves at different temperatures is better.

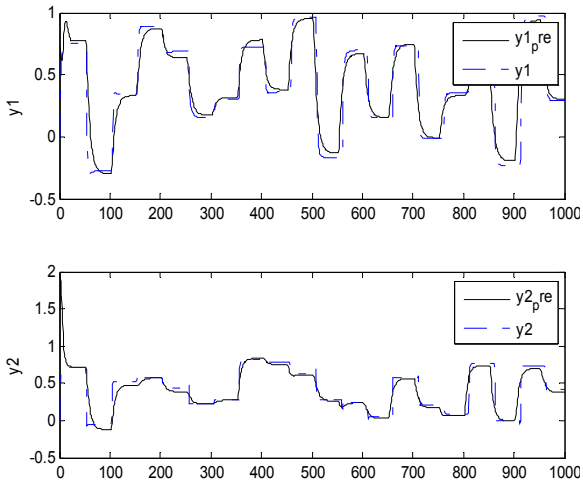

Fig. 6. The results of PLS dynamic modeling.

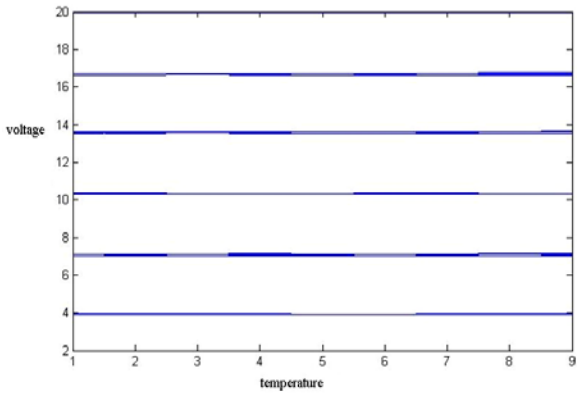

Fig. 7. Simulation results of the system.

We can get the he experimental results analysis by the data in Table 3, and Table 4.

1) The experiment measured data is obtained in the warming case, the residence time at each measurement point is 30 minutes, this case is consistent with algorithm compensation temperature, the real objective compensation effect can be reflected objectively to a certain extent.

2) It can be found that the algorithm has significant improvement for sensitivity drift by contrasting Zero drift and sensitivity drift data before and after sensor compensation, sensitivity temperature drift error has been reduced on the order of magnitude.

3) The entire compensation circuit is in the -40 °C~100 °C temperature range, the linearity of curves at different temperatures is better.

5. Conclusion

This paper proposes temperature compensation model based on principal component analysis against the existence of the defect for the slow convergence of principal component analysis in the wrist sensor temperature compensation, and simulates compensation for the wrist sensor temperature drift of the model.

References

[1]. Xu Kejun, Practical study method of dynamic characteristics of sensor, *University of Science & Technology China Press*, 1999.

[2]. Wang Guotai, *et al.*, Several problems in the development of six axis force sensor, *The Robot*, Vol. 19, Issue 6, 1997, pp. 474-478.

[3]. Xu Kejun, Li Cheng, Study on static decoupling of multidimensional wrist force sensor, *Journal of HeFei University of Technology*, Vol. 22, Issue 2, 1999, pp. 1-6.

[4]. Wu Juan, Study on the improvement and robot modeling six dimension wrist force sensor, *Master's Degree Thesis of Southeast University*, 2002.

[5]. Liu Zhengshi, The system error analysis of six component wrist force sensor loading test bench of robot, *Acta Metrologica Sinica*, Vol. 19, Issue 1, 1998, pp. 44-51.

[6]. Wang Yaodong, Dynamic calibration of robots wrist force sensor, *Master's Degree Thesis of Southeast University*, 1990.

[7]. Xu Kejun, Zhu Nengcheng, Li Cheng, Experimental modeling of six dimension wrist force sensor step response, *The Robot*, Vol. 22, Issue 4, 2000, pp. 251-225.

[8]. Liu Zhengshi, Study on the dynamic load effect of robot wrist force sensor, *The Robot*, Vol. 20, Issue 3, 1998, pp. 181-186.

[9]. Wold S., M. Sjöström, *et al.*, PLS-regression: a basic tool of chemometrics, *Chemometrics and Intelligent Laboratory Systems*, Vol. 58, Issue 2, 2001, pp. 109-130.

[10]. Wang Huiwen, Linear and nonlinear approach of partial least square regression, *National Defence Industry Press*, Beijing, 2006.

[11]. Chen J., Fang W., PLS based dEWMA run-to-run controller for MIMO non-squared semiconductor processes, *Journal of Process Control*, Vol. 17, 2007, pp. 309-319.

[12]. Zhao Z., Hu B., Liang J., Multi-loop adaptive internal model control based on a dynamic partial least squares model, *Journal of Zhejiang University-SCIENCE A*, Vol. 12, Issue 3, 2011, pp. 190-200.